Pyrolysis kinetic modelling of abundant plastic waste (PET) and in-situ emissions monitoring

Ahmed I. Osman (aosmanahmed01@qub.ac.uk)
Queen's University Belfast Faculty of Engineering and Physical Sciences https://orcid.org/0000-0003-2788-7839

Charlie Farrell
Queen's University Belfast Faculty of Engineering and Physical Sciences

Ala'a H. Al-Muhtaseb
Sultan Qaboos University

Ahmed S. Al-Fatesh
King Saud University

John Harrison
SOUTH WEST COLLEGE

David W. Rooney
Queen's University Belfast Faculty of Engineering and Physical Sciences

Research

Keywords: Kinetic modelling, Plastic waste, Pyrolysis, Polyethylene terephthalate, Gaseous emissions, Plastic recycling

Posted Date: August 17th, 2020

DOI: https://doi.org/10.21203/rs.3.rs-29640/v2

Version of Record: A version of this preprint was published on August 31st, 2020. See the published version at https://doi.org/10.1186/s12302-020-00390-x.

Abstract

Background: Recycling the ever-increasing plastic waste has become an urgent global concern. One of the most convenient methods for plastic recycling is pyrolysis, owing to its environmentally friendly nature and its intrinsic properties. Understanding the pyrolysis process and the degradation mechanism is crucial for scale-up and reactor design. Therefore, we studied kinetic modelling of the pyrolysis process for one of the most common plastics, polyethylene terephthalate (PET). The focus was to better understand and predict PET pyrolysis when transitioning to a low carbon economy and adhering to environmental and governmental legislation. This work aims at presenting for the first time, the kinetic triplet (activation energy, pre-exponential constant and reaction rate) for the PET pyrolysis using the differential iso-conversional method. This is coupled with the *in-situ* online tracking of the gaseous emissions using mass spectrometry.

Results: The differential iso-conversional method showed activation energy (E_a) values of 165-195 kJ.mol^{-1}, R^2 = 0.99659. While the ASTM-E698 showed 165.6 kJ.mol^{-1} and integral methods such as Flynn-Wall and Ozawa (FWO) (166-180 kJ.mol^{-1}). The *in-situ* Mass Spectrometry results showed the pyrolysis gaseous emissions which are C_1-hydrocarbon and H-O-C=O along with C_2 hydrocarbons, C_5- C_6 hydrocarbons, acetaldehyde, the fragment of O-CH=CH_2, hydrogen and water.

Conclusions: From the obtained results herein, thermal predictions (isothermal, non-isothermal and step-based heating) were determined based on the kinetic parameters and can be used at numerous scales with a high level of accuracy compared with the literature.

Background

Over nine billion tonnes of plastic have been produced globally since the 1940s, with an annual growth rate of 8.7% [1]. Plastic materials are subdivided into seven different types and fulfil different purposes in our daily life such as in electronics, construction materials, agriculture, household items and packaging films. The widespread use is due to their intrinsic properties i.e. chemical inertness, mechanical, pressure resistance, durability, versatility, flexibility, cheap production cost, along with the thermal stability from the additives and stabilisers used in the production phase [2]. Over the last 60 years, consumer plastic use has increased by approximately 20 times, where the annual production has dramatically increased from 15 million tonnes (Mt) in 1964, to 335 Mt in 2016, and is expected to reach 1124 Mt by the year 2050 [3, 4]. The annual consumption of water bottles alone has reached 500 billion units globally [5]. However, the disposal rate of these plastic debris has risen, making a huge negative impact on the environment as well as public human health. The plastic waste generated in 2015 was 6300 Mt, where only 9% has been recycled, 12% incinerated and the rest have been sent to landfills (79%) [6]. In the next five years, the plastic waste production rate will reach 220 Mt per annum, with its end-of-life destination deemed to be mainly in the sediment, biota and aquatic ecosystem such as oceans and rivers (micro-plastic (<5mm), nanoplastic (<1.2μm)), [7] where the complete degradation of its polymers could take centuries. Furthermore, direct burning of those plastic wastes generates hazardous emissions along with chemicals

such as phosgene, dioxins, and carbon monoxide that are linked to human cancers and endocrine disruption [8, 9]. However, it is possible to add additional value to this waste through processes such as pyrolysis, solvent dissolution, gasification and other valorisation approaches whilst promoting the circular economy [10, 11]. This approach of using a waste stream will complete the full cycle of plastic and thus, directly support and facilitate the concept of the circular economy.

There are mainly four different technologies in dealing with plastic waste management which are: re-extrusion that requires semi-clean plastic scrap, along with mechanical (physical), chemical (solvolysis and pyrolysis) and energy recovery (incineration) [2, 12, 13]. For instance, Lopez et al. investigated the thermochemical routes for the production of value-added products (fuel and chemical) via the valorisation of waste poly-olefinic plastics. They found out that the variability and inconsistency of the feed composition was the majour challenge along with catalyst deactivation [14-16].

The most common polymers studied are polyethylene terephthalate (PET), High-density polyethylene (HDPE), polypropylene (PP) and polystyrene (PS), where the pyrolysis and reforming conditions were around 500 and 700 °C, respectively. Nearly half of the total plastic market globally comes from PE (polyethylene) and PET with a contribution of 40% [17] in various sectors such as agriculture, drinking water bottles, food packaging and constructional materials. Thermoplastics account for 80% of the total plastic consumption [2]. PET ($(C_{10}H_8O_4)_n$) is the most abundant thermoplastic due to its characteristics to exist in different forms such as a one-dimensional fibre, 2D-films and 3D-bottles and containers [18, 19]. It is the third-most consumed polymer in Europe after PP and LDPE, and the most widely used plastic in the packaging industry [20-22]. The global consumption and demand for PET reached 60 Mt by 2011 and is increasing by 4.5% each year [23]. It has been reported in the literature that PET plastic material has a similar energy content than that of soft coal, with a higher heating value of 46.2 $MJ.kg^{-1}$ and ultimate elemental analysis of >45 wt.% carbon, 36 wt.% hydrogen and 18 wt.% oxygen [20, 24, 25]. Most of those PET and plastic waste materials, in general, are non-biodegradable and their end-of-life destination is landfill or incineration. There is also another challenge that faces the recycling of these problematic materials, which is the difficulty of the selective and effective separation of the plastic mixture. For instance, a standard PET bottle contains about 10-15 wt.% PE in the form of printed labels and cups, where their separation is usually difficult [17].

One of the most convenient methods for plastic recycling is pyrolysis owing to its environmentally friendly nature. Furthermore, unlike other recycling processes such as mechanical and chemicals methods, pyrolysis is a flexible process where plastic waste could be treated alongside municipal solid waste such as e-waste, biomass and others [26]. Interestingly, only 5% of the calorific value of the plastic waste is being used in the endothermic cracking process, which in the case of PET is 214 $kJ.kg^{-1}$ [27]. The pyrolytic products of plastic are oil (22-49 wt.%), gases (18-30 wt.%), and solid char (30-50 wt.%); where different operating parameters could affect the process and product composition (plastic-type, residence time, pyrolytic temperature, ramping rate and reactor type) [27]. As the operating parameters can shift the product composition and alter the reaction pathway, it is important to use kinetic modelling to help describe the reaction mechanism during the thermal cracking of plastic polymers. Ganeshan et al. [28] in

their attempt to understand the PET pyrolysis process via kinetic modelling, used Coats–Redfern method that assumes the reaction is first order. They reported activation energies (E_a) value in the range of 133-251 kJ.mol^{-1}, however, the value of R^2 was low (<0.8). Thus, they concluded that the Coats–Redfern method is not always suitable for calculating the kinetic parameters. Mishra et al.[29] studied kinetic modelling approaches (Coats-Redfern method, Kissinger-Akahira-Sunose, Flynn-Wall and Ozawa method, Friedman method and Starink) for the co-pyrolysis of PET with biomass seeds. The KAS method of PET pyrolysis showed variation in the E_a value from 210-241 kJ.mol^{-1} within reaction progress α = 0.1-0.8, where the average E_a was 230.7 kJ.mol^{-1}. Under the same conditions, the FWO and Starink methods showed similar variation in the E_a value from 211-241 kJ.mol^{-1} and 211-242 kJ.mol^{-1}, respectively with an E_a average of 230.5 and 231.0 kJ.mol^{-1}. The Friedman method showed slightly lower variation in values under the same conditions with 208.6-236 kJ.mol^{-1} and an average E_a of 225.6 kJ.mol^{-1}. They performed the kinetic modelling based on three heating rates of 10, 30 and 50 °C.min^{-1}, while for reliable evaluation of the kinetic parameters, it should be at low heating rates of less than 8 °C.min^{-1} (with a ratio between the lowest and the highest heating rate of >10) with four or five heating rates [30]. Das and Tiwari [18] measured the kinetic parameters for PET pyrolysis at high heating rates of 5, 10, 20, 40 and 50 °C.min^{-1} using the iso-conversional method. They reported E_a values in the range of 196-217 kJ.mol^{-1}. Al-asadi and Miskolczi measured the emissions related to the uncatalysed along with Ni/zeolite catalytic pyrolysis of PET but only at a high-temperature range of 600-900 °C [17]. To the best of the authors' knowledge, this is the first detailed study in measuring and evaluating the kinetic triplet (activation energy, pre-exponential constant and reaction rate) of PET plastic pyrolysis with the use of Advanced Kinetics and Technology Solutions (AKTS) software. This work aims at presenting for the first time, the kinetic triplet (activation energy, pre-exponential constant and the rate of reaction) for the PET pyrolysis using the differential iso-conversional method. This is coupled with the *in-situ* online tracking of the gaseous emissions using mass spectrometry, as there are few and limited studies on oxygenated macromolecules such as PET in the literature [20, 22]. The kinetic triplet can benefit in process modelling systems to help better understand the process at scale, as these values are not influenced based on scale.

Materials And Methods

Sample preparation and In-situ gaseous emission detection using Mass Spectrometry

The PET sample was collected from used water bottles, then washed with deionised water, dried and finally crushed down into a form of small particles and sieved in the range of less than 100 μm to avoid the mass and heat transfer limitations during the kinetic modelling and pyrolysis tests as shown in Figure S1. The PET pyrolysis was performed in a fixed bed reactor, where the output of the reactor is coupled and attached to a mass spectrometer (MS) through a heated quartz capillary tube. To prevent any condensation, dissolution or adsorption on the tube wall, all the lines were heated to 150 °C, where the evolved gas mixtures were then directly fed to the mass spectrometer. The MS (Hiden Analytical instrument) was performed under vacuum and the rapid *in-situ* detection of the characteristic fragment

ion intensity of the associated gaseous emissions such as hydrocarbons and other related emissions including characteristic ion species according to its mass to charge ratio (*m/z*) such as *m/z* = 15 (C_1 hydrocarbons), *m/z* = 27 (C_2 hydrocarbons), *m/z* = 42 (C_5 hydrocarbons), *m/z* = 78 (C_6 hydrocarbons), *m/z* = 84 (Krypton), *m/z* = 43 (acetic acid), *m/z* = 44 (acetaldehyde or carbon dioxide), *m/z* = 2 (hydrogen), *m/z* = 45 (CHO_2), *m/z* = 18 (water) and *m/z* = 29 (acetaldehyde).

Kinetic modelling of PET Waste via AKTS:

The evaluation of the kinetic parameters of the PET pyrolysis was determined using the TGA data (at different heating rates of 0.5, 1, 2, 4, and 8 °C.min^{-1}) under N_2 atmosphere with a ratio of 16 between the lowest and the highest heating rate. The heating rate of 4 °C.min^{-1} was repeated for the reproducibility and accuracy of results. The TGA experiments were conducted in a simultaneous thermal analysis Mettler Toledo (TGA/DSC) Thermogravimetric analyser Pyris TGA/DSC1, changes in the mass of the sample were recorded during the ramping operation.

The TGA instrument was also calibrated for buoyancy effects to allow quantitative estimation of weight changes. Experiments were performed twice to ensure reproducibility and the standard error was found to be ±1 ºC. The ICTAC Kinetics Committee published the problems and reporting the essential principals that should be followed to obtain thermal analysis data that are adequate to the kinetic computations [31]. To determine the kinetic parameters more accurately and to better understand the PET pyrolysis, Advanced Kinetics and Technology Solutions (AKTS) software utilised. AKTS software correlated and validated the practical experiments with theoretical calculations for the kinetic modelling of the pyrolysis process of the PET plastic waste along with calculating the activation energy (E_a) and the pre-exponential factor. Different kinetic modelling methods were employed such as ASTM-E698, Flynn-Wall and Ozawa (FWO), and differential iso-conversional (model-free) method such as the Friedman method. The latter method measures E_a and pre-exponential constant at different extents of reaction progress α without requiring prior knowledge of the reaction mechanism [32]. Consequently, the iso-conversional method was used herein to measure the kinetic parameters using heating rates ranging from 0.5 to 8 °C.min^{-1} as a function of reaction progress (α). Where the rate of the thermal decomposition of the waste PET plastic can be expressed according to the iso-conversional method as a function of reaction temperature and α, where the latter is calculated from the initial, actual and final masses of PET waste. The Arrhenius equation defined the temperature-dependent function of the kinetic parameters as shown below in Equation 1. (see Equation 1 in the Supplementary Files)

The non-isothermal iso-conversional method usually utilizes different heating rates, β = dT.dt $^{-1}$, thus the PET plastic pyrolysis can be expressed as in Equation 2 as shown below: (see Equation 2 in the Supplementary Files)

One of the examples of iso-conversional methods (the non-isothermal) such as ASTM-E698 as shown in Equation 3 below: (see Equation 3 in the Supplementary Files)

Whereas the Flynn-Wall and Ozawa (FWO) method is shown in Equation 4 as shown below: (see Equation 4 in the Supplementary Files)

The equation for the Kissinger-Akahira-Sunrose (KAS) methods is shown below in Equation 5:(see Equation 5 in the Supplementary Files)

Finally, the isothermal iso-conversional method is represented in the Friedman method as shown below in Equation 6:(see Equation 6 in the Supplementary Files)

Results And Discussion

The kinetic modelling results:

AKTS thermokinetics package was utilised in this study to facilitate kinetic analysis of PET plastic bottle samples using conventional thermoanalytical data; which in the case of this study was in the form of TGA. This can allow for the study of the thermal behaviour of the PET samples within the discrete areas of quality assurance and research and development (R&D). The analysis begins with the importations of ASCII files from the TGA instrument. A derivation filter is then applied to provide the DTG reading of the sample. The DTG signal then has a baseline constructed in order to integrate the curve and provide the evaluation of the kinetic parameters such as rate of reaction, activation energy and pre-exponential constant (also commonly known in the literature as the kinetic triplet). Herein, baselines were constructed to integrate the DTG results with respect to the PET plastic pyrolysis profile. The type of baseline used herein was horizontal. AKTS has numerous possibilities for advanced baseline construction such as spline, sigmoid, tangential first point, tangential last point etc. as baseline construction is the most crucial step in kinetic data treatment and these constructed baselines can be optimised numerically. Additionally, the parameters for the Arrhenius equation can be determined for multi-step complex reactions, which cannot be visually seen if the thermoanalytical curves potentially overlap. Based on the obtained kinetic parameters, simulation curves are generated for the reaction rate and the reaction progress which were compared with the experimental data to check the accuracy of the modelling. As the PET pyrolysis reaction progress, there is a change in the specific heat of the reactant-products mixture, thus changing the heat of reaction and consequently the kinetic parameters. Specifically using the AKTS package the progress/extent of reaction (α) and the reaction rate can be predicted for a wide variety of temperature profiles (non-isothermal, isothermal, modulated or periodic temperature variations or step base heating.

The software ultimately provides a robust and accurate result due to strict thermokinetic criteria of average correlation coefficient R having to be greater than 0.95 and the plotting of high-resolution data over 10,000 specific data points for the parameters and alpha values. Figure S2 shows the practical results, their integration, and the subsequent simulated results from the TGA kinetic modelling results at different heating rates from 0.5 to 8 °C.min^{-1}. Similar TGA results were reported in the literature [22, 27, 33, 34]. The high mass loss in PET pyrolysis is due to the high volatile matter content as reported by Lee et al. , who reported a value of 86.1 wt.% [22], Oh et al. was 88.1%[25], while Park et al. stated 91.6% [34]

in PET pyrolysis. While the DSC results of two heating rates (0.5 and 1 °C.min^{-1}) showed two endothermic peaks, along with a small shoulder of an exothermic peak as shown in Figure S3. The first two endothermic peaks at 252 and 460 °C are due to the PET melting and pyrolysis, while the third peak at around 800 °C is characteristic to the graphitization of the residual carbon material. This agrees with the work reported by Kamali et al. where the three peaks appeared at 254, 466 and 791 °C respectively [5]. It is obvious that there is a good match between the practical and theoretical simulation as shown in Figure S2 from the lowest to the highest heating rate with R^2 = 0.99659.

Table 1. The thermogravimetric decomposition data of PET plastic pyrolysis at various heating rates from 0.5 to 8 °C.min^{-1}.

Heating rates	0.5 °C.min^{-1}	1 °C.min^{-1}	2 °C.min^{-1}	4 °C.min^{-1}	8 °C.min^{-1}
Temperature (°C)	261-442	284-455	284-485	321-509	328-535
Time required (s)*	49,447	25,502	13,650	7,190	3,789
Peak maximum (°C, s^{-1})	374,4.1 x 10^4	389,2.2 x 10^4	402,1.1 x 10^4	417,5.8 x 10^3	433,3.0 x 10^3
Peak height (%.min^{-1})	1.1	2.4	5.0	9.7	19.7
Onset temperature (°C)	351	366	394	399	413
Offset temperature (°C)	397	412	421	432	453

* Time required for complete reaction (s).

There is a clear shift towards a higher decomposition temperature by increasing the heating rate 16 times (from 0.5 to 8 °C.min^{-1}) as shown in Table 1 with R^2 = 0.99659. For instance, the temperature range for the pyrolysis reaction to occur at 0.5 °C.min^{-1} was 261-442 °C, while at 8 °C.min^{-1}, it increased to 328-535 °C. Furthermore, the onset temperature increased from 351 to 413 °C, respectively. By increasing the heating rates by 16 times, the offset temperature increased by 56 °C as shown in Table 1. Thus, it is not surprising that the peak maximum was shifting towards higher reaction temperature with increasing the heating rates, as 0.5, 1, 2, 4 and 8 °C.min^{-1} showed peak maximum at 374, 389, 402, 417 and 433 °C, respectively. On the other hand, the time required for the pyrolysis reaction to finish has dramatically decreased by 13 times with increasing the heating rates by 16 times. Table 1 shows that the required time for completion at 0.5 °C.min^{-1} was 49447 seconds, while at 8 °C.min^{-1} was 3789 seconds. Based on the integrated DTG curves from the five heating rates shown in Figure S2, the average PET plastic weight loss up to 600 °C was 82.898 ± 1.2 wt.% of its initial mass.

To obtain the kinetic parameters, first, the reaction progress (α) was plotted versus the reaction temperature as shown in Figure 1, where the practical and theoretical results are shown in coloured and dashed-grey lines, respectively. Again, it is obvious that there is a good matching between practical and theoretical results.

Figure 2 shows the practical and theoretical reaction rate against reaction temperature, where the coloured and dashed grey curves show the practical and theoretical calculations, respectively, with good matching in all the five heating rates. The maximum reaction rate of the PET pyrolysis at heating rates of 0.5, 1, 2, 4 and 8 °C.min^{-1} were found to be 0.000089, 0.000449, 0.00092, 0.00188 and 0.00386 s^{-1}, respectively. Thus, the reaction rate increased by approximately 43 times with increasing the heating rates by 16 times i.e. from 0.5 to 8 °C.min^{-1}.

One of the kinetic modelling methods, ASTM-E698 (Equation 3) was used to calculate the E_a and showed 165.6 kJ.mol^{-1} with R^2 = 0.9989 as shown in Figure 3 (a). This in agreement with the E_a value reported by Saha and Ghoshal which was 162.15 kJ.mol^{-1} using the ASTM-E698 method [35].

While the Flynn-Wall and Ozawa (FWO) method (Equation 4) showed a variation of E_a during the reaction progress in the range of 166-180 kJ.mol^{-1} as shown in Figure 3 (b). The results herein are lower than that reported by Yao et al. [36], who reported 184-269 kJ.mol^{-1}. This is maybe due to the fact that they did not specify the plastic waste that they used along with the high heating rates used (15, 25 and 35 °C.min^{-1}).

The differential iso-conversional method also was used to calculate the kinetic parameters (Ea along with the pre-exponential factor (k_o)) using the AKTS software by plotting of the natural logarithm of the reaction rate in (s^{-1}) against the inverse of the temperature (T^{-1}) as shown in Figure 4 (a). In Figure 4 (b) a variation in the E_a value was shown to be in the range of 165-195 kJ.mol^{-1}. Interestingly, the results herein are in line with the work done by Jenekhe and Sun, where they reported E_a values of 173.6 – 205.8 kJ.mol^{-1} using the iso-conversional method [37]. At the start of the PET pyrolysis reaction where α=0, the activation energy was 165 kJ.mol^{-1}. This is in agreement with work done by Cooney and Wiles [38], where the E_a value of the initial pyrolysis stage using Kissinger's Method was 163 kJ.mol^{-1}. This activation energy value stayed relatively constant while the reaction progress was increasing up to α=0.3 i.e. 30% of the reaction progress, while the pre-exponential factor; ln(A(α) f(α) is ~ 22 s^{-1}. This high E_a value at the start of the pyrolysis reaction could be attributed to the depolymerization of the polyethylene terephthalate polymer, which requires high energy to cleave the bonding within the polymer structure for the PET pyrolysis reaction, to initiate and progress. With the pyrolysis reaction progressing > α=0.3, the activation energy value slightly increased to reach 195 kJ.mol^{-1} at α=0.9, while the pre-exponential factor; ln(A(α) f(α) is ~ 26 s^{-1}. This is again, in-line with the work reported by Cooney and Wiles [38], where the E_a value increased to 202 kJ.mol^{-1}.

The prediction of PET pyrolysis

The step-based prediction of PET pyrolysis

The predictions of PET pyrolysis using a step-based heating regime are shown in Figure 5 (a-d). For all four predictions, the final pyrolysis temperature was set to 500 °C, as this was in line with total

decomposition from the TGA results. Additionally, all heating regimes began at 20 °C to indicate heating from ambient room temperature. In Figure 5a, the PET was heated from 20-420 °C at 50 °C.min^{-1} and then from 420-500 °C at 25 °C.min^{-1}. It is evident that the reaction had appeared to complete after 11 minutes from the reaction rate curve. Interestingly, the maximum reaction rate observed was 0.014 s^{-1} at approximately 9.77 minutes. In Figure 5b, the heating regime of 20-400 °C at 100 °C.min^{-1} and 400-500 °C at 50 °C.min^{-1} was utilised. For this sample condition, the peak reaction rate was shown to be 0.029 s^{-1} after approximately 5.42 minutes. From the reaction rate curve, it can be seen that the curve does not reach its baseline of 0 and is incomplete, therefore, implying an incomplete reaction. This is likely due to the heating rates used of 100 and 50 °C.min^{-1}, respectively. If the reaction had occurred for longer at 50 °C.min^{-1} or dwelled at the final reaction temperature of 500 °C, it would have reached completion. Figure 5c, on the other hand, is subjected to a heating regime of 100 °C.min^{-1} from 20-320 °C and then 20 °C.min^{-1} from 320-500 °C, respectively. However, in this case, the lower latter heating rate supplied allowed the observed reaction to reach completion. In this instance, the peak reaction rate observed was 0.010 s^{-1} after 9.86 minutes. Finally, Figure 5d was heated from 20-450 °C at a heating rate of 100 °C.min^{-1} and then from 450-500 at a heating rate of 5 °C.min^{-1}. The maximum observed reaction rate was 0.011 s^{-1} after 5.42 minutes. Interestingly, the curve in this sample appeared to have a shoulder and this is likely due to the rapid change in heating rate from 100 to 5 °C.min^{-1}, respectively.

Isothermal prediction of PET pyrolysis

The isothermal prediction of PET pyrolysis showing 14 different isotherms at every 10 °C temperature change over the temperature range of 420-550 °C is shown in Figure 6 (a, b). Figure 6a shows the reaction progress over the first minute, whereas Figure 6b shows the reaction profile over the first five minutes. Evidently, from Figure 6a, at reaction temperatures of 490 °C and above, the reaction reached completion, (α=1) in the short timeframe of one minute. This rapid decomposition indicates that these temperatures would be ideal for rapid conversion. However, at lower than 490 °C, for example, 480, 470 and 460 °C, the reaction progress only reached α values of 0.93, 0.81 and 0.55, respectively after the first minute. As Figure 6b shows the decomposition over a broader time range, it is worth noting that temperatures such as 450-480 °C that did not reach (α=1) in Figure 6a, have reached reaction completion when the timeframe is expanded to five minutes of operation. Below 450 °C shows a much slower reaction and indicates that the reaction has not reached completion in this case. This further indicates that in order for successful pyrolysis to occur of PET temperatures exceeding 450 °C should be used.

Non-isothermal prediction of PET pyrolysis

Figure 7 shows the non-isothermal prediction of PET pyrolysis over the temperature range of 350-500 °C. It is not surprising that the decomposition temperature shifted slightly toward higher reaction temperature. For example, by increasing the heating rates from 10 up to 30 °C.min^{-1}, the peak reaction rates observed were 0.0051, 0.0077, 0.0104, and 0.0159 s^{-1}, respectively. In all four heating rates

used (10, 15, 20 and 30 °C.min^{-1}) for the prediction, the reaction profile and reaction rate curves appeared to be consistent.

The *in-situ* gaseous monitoring of PET pyrolysis

During the pyrolysis process, two main reactions occur: cracking which breaks down the carbon chain and the charring reaction which aids to re-build up higher molecular weight products [39]. For instance, polyolefins (PP and HDPE) are composed of a saturated hydrocarbon chain, where the thermal decomposition takes place randomly by radical scission mechanism [40, 41]. However, due to the aromatic nature of PS, it decomposes into styrene monomers (70.6 wt.%), oligomers and other secondary aromatic products. On the other hand, PET is composed of terephthalic acid and ethylene glycol monomers, thus upon pyrolysis, various oxygenates and aromatics products are produced. The pyrolysis residue in the case of polyolefins was negligible, unlike PET that showed a value of 7 wt.% residue [40]. Barbarias et al. reported that the main PET pyrolysis fraction was a gaseous stream (CO and CO_2), with a product yield of 42.8 wt.%, along with 37.4 wt.% for the solid residue (benzoic and benzoyl formic acid) and 12.8 wt.% for oil fraction. The PET plastic consists of chain-like backbones of synthetic polymers that are made of bis-hydroxyethyl-terephthalate monomer and with thermal cracking or pyrolysis, it evolved various gaseous emissions. The PET pyrolysis is a complex process that releases different types of products such as aromatic compounds, such as benzene and toluene and aliphatic hydrocarbons C_1-C_4 such as methane and ethane along with the typical pyrolytic emissions (CO_2, CO, H_2 and H_2O) [20, 42-44]. Furthermore, other species could be released such as aldehydes, carboxylic acids (benzoic acid, acetyl benzoic acid, methyl benzoic acid and ethyl benzoic acid), esters (vinyl benzoate and its derivatives), ketones (benzophenone and acetophenone) and terephthalic acid and vinyl terephthalate [20, 45-47]. The complexity of such reaction is due to the possibility of several side interactions between free radicals during the scission of the polymeric hydrocarbon chain such as intramolecular or intermolecular exchange and six-membered transition state reactions [27]. Figure 8 shows the *in-situ* monitoring of the evolved gaseous emissions using the mass spectrometer which offers rapid analysis and is not limited to the shape, colour, impurities or dimensional limit as in other techniques such as Fourier-transform infrared spectroscopy (FTIR) and Raman spectroscopy [1]. Herein, the temperature was recorded using a thermocouple that was set in the middle of the fixed bed reactor as shown from the blue-dashed line in Figure 8. The PET pyrolysis herein occurred in one stage, which is in line with the TGA results with a similar heating rate, while the DSC results in Figure S3 showed that the pyrolysis occurred in two stages. Figure 8 shows the pyrolysis reaction was in the temperature range of 390-500 °C, while the TGA result was in the range of 382-490 °C (heating rate of 4 ^{o}C.min^{-1}). The *in-situ* MS data showed that the main emissions are C_1-hydrocarbons at *m/z* =15 and H-O-C=O (CHO_2) at *m/z* =45. The *in-situ* MS profile also showed some relatively low emissions as shown from the inset (Figure 8), that showed the evolution of various forms of hydrocarbons such as C_2 hydrocarbons at *m/z* = 27, C_5 hydrocarbons at *m/z* = 42 and C_6 hydrocarbons at *m/z* = 78. Furthermore, other related emissions were shown as acetaldehyde or carbon dioxide at *m/z* = 44, the fragment of O-CH=CH_2 at *m/z* = 43, hydrogen gas at *m/z* = 2, water at *m/z* = 18 and finally, *m/z* = 29 that confirms the existence of acetaldehyde as following the

same trend as with *m/z* = 44. This is in agreement with the work done by Garozzo et al. as they reported the presence of the O-CH=CH_2 fragment and m/z of 17 for -OH species that confirmed the metastable transitions of the fragments, implying the existence of the open-chain structure with C(=O)O and −CH=CH_2 groups [48]. Acetaldehyde was the first gaseous product that evolved and finished as shown in Figure 8, this was confirmed by the *m/z* = 44 and 29 with the same evolution trend. This is in line with the work reported by Dhahak et al. [20], as they reported that acetaldehyde was the first detected gas followed by the following gases; benzoic acid, terephthalic acid, and benzene. Traces of benzene was detected herein in two peaks as shown in Figure S4, with a large peak and small shoulder. This is also in agreement with the literature, as it was explained that those two peaks are due to the decarboxylation of benzoic acid (1st peak) and terephthalic acid (2nd peak) [33]. Dhahak et al. reported that the major three gaseous compounds detected during the pyrolysis of PET were acetaldehyde, benzoic acid and vinyl terephthalate [20]. During the PET pyrolysis, the depolymerisation reaction starts to occur at the weak bonding points within the ester polymeric structure, such as the C-O bonding and the polymer chain near the C=O bonding [27]. It is worth noting that the evolved short-chain hydrocarbon (C_1-C_4 hydrocarbons) emissions can be combusted to provide some of the required reaction heat during the pyrolysis process [27].

Conclusions

Herein, with the aid of thermo-analytical data (TGA and DSC) along with kinetic modelling software, we evaluated and measured the kinetic triplet of polyethylene terephthalate pyrolysis to better understand the process at scale. Furthermore, three types of predictions (step prediction, non-isothermal and isothermal) were made at higher heating rates to represent a realistic scenario that would occur in the industry. The differential iso-conversional method showed activation energy (E_a) values of 165-195 kJ.mol^{-1}, R^2 = 0.99659. Additionally, the activation energy for PET pyrolysis was also evaluated using the ASTM-E698 (165.6 kJ.mol^{-1}, R^2 = 0.9989) and integral methods such as Ozawa-Flynn-Wall (166-180 kJ.mol^{-1}). Future work could involve the use of kinetic modelling approaches such as the methods used herein to help determine how certain impurities or mixed wastes alongside PET can affect kinetic parameters and the predictions made in this study to help visualise problems that may occur in real-world scenarios such as industrial pyrolysis processes. This work can be used as a baseline kinetic modelling benchmark for pure PET bottle samples. The kinetic parameters evaluated herein can be used as a prerequisite in process modelling applications and the scale-up of PET pyrolysis worldwide. This will effectively allow this abundant waste stream to be converted into useful products such as energy and help promote concepts such as the circular economy and the waste management hierarchy. Additionally, it will alleviate the amount of waste plastic that is conventionally sent to landfill or end in the aquatic ecosystem, by providing another end-of-life pathway for this non-biodegradable waste.

Abbreviations

polyethylene terephthalate (PET), Flynn-Wall and Ozawa (FWO) method, activation energy (E_a) and million tonnes (Mt).

Declarations

Acknowledgements: The authors would like to acknowledge the support UKRI project “Advancing Creative Circular Economies for Plastics via Technological-Social Transitions” (ACCEPT Transitions, EP/S025545/1).

Author Contribution: A.I.O. conceived the idea, prepared, and tested the PET pyrolysis. A.I.O, C.F, A.H.M, A.S.A, J.H and D.W.R extracted and discussed the kinetic modelling and emission tests. All authors discussed and contributed to the writing of the paper.

Competing interests: The authors declare no competing interests.

Ethics approval and consent to participate: Not applicable

Consent for publication: Not applicable

Availability of data and material: The data and results obtained herein are available from the corresponding author on reasonable request.

Funding: The research is funded through UKRI project “Advancing Creative Circular Economies for Plastics via Technological-Social Transitions” (ACCEPT Transitions, EP/S025545/1).

References

[1] X. Zhang, H. Zhang, K. Yu, N. Li, Y. Liu, X. Liu, H. Zhang, B. Yang, W. Wu, J. Gao, J. Jiang, Rapid Monitoring Approach for Microplastics Using Portable Pyrolysis-Mass Spectrometry, Analytical Chemistry, 92 (2020) 4656-4662.

[2] S.M. Al-Salem, P. Lettieri, J. Baeyens, Recycling and recovery routes of plastic solid waste (PSW): A review, Waste Management, 29 (2009) 2625-2643.

[3] M. Wagner, M. Engwall, H. Hollert, Editorial: (Micro)Plastics and the environment, Environmental Sciences Europe, 26 (2014) 16.

[4] N. Beagan, K.E. O’Connor, I.J. Del Val, Model-based operational optimisation of a microbial bioprocess converting terephthalic acid to biomass, Biochemical Engineering Journal, 158 (2020) 107576.

[5] A.R. Kamali, J. Yang, Q. Sun, Molten salt conversion of polyethylene terephthalate waste into graphene nanostructures with high surface area and ultra-high electrical conductivity, Applied Surface Science, 476 (2019) 539-551.

[6] R. Geyer, J.R. Jambeck, K.L. Law, Production, use, and fate of all plastics ever made, Science Advances, 3 (2017) e1700782.

[7] J. Zhang, Q. Hu, Y. Qu, Y. Dai, Y. He, C.-H. Wang, Y.W. Tong, Integrating food waste sorting system with anaerobic digestion and gasification for hydrogen and methane co-production, Applied Energy, 257 (2020) 113988.

[8] F. Gallo, C. Fossi, R. Weber, D. Santillo, J. Sousa, I. Ingram, A. Nadal, D. Romano, Marine litter plastics and microplastics and their toxic chemicals components: the need for urgent preventive measures, Environmental Sciences Europe, 30 (2018) 13.

[9] B. Zhang, T. Xu, D. Yin, S. Wei, The potential relationship between neurobehavioral toxicity and visual dysfunction of BDE-209 on zebrafish larvae: a pilot study, Environmental Sciences Europe, 32 (2020) 25.

[10] L. Xu, L.-y. Zhang, H. Song, Q. Dong, G.-h. Dong, X. Kong, Z. Fang, Catalytic fast pyrolysis of polyethylene terephthalate plastic for the selective production of terephthalonitrile under ammonia atmosphere, Waste Management, 92 (2019) 97-106.

[11] C.C. Farrell, A.I. Osman, R. Doherty, M. Saad, X. Zhang, A. Murphy, J. Harrison, A.S.M. Vennard, V. Kumaravel, A.H. Al-Muhtaseb, D.W. Rooney, Technical challenges and opportunities in realising a circular economy for waste photovoltaic modules, Renewable and Sustainable Energy Reviews, 128 (2020) 109911.

[12] V. Sinha, M.R. Patel, J.V. Patel, Pet Waste Management by Chemical Recycling: A Review, Journal of Polymers and the Environment, 18 (2010) 8-25.

[13] X. Zhou, C. Wang, C. Fang, R. Yu, Y. Li, W. Lei, Structure and thermal properties of various alcoholysis products from waste poly(ethylene terephthalate), Waste Management, 85 (2019) 164-174.

[14] G. Lopez, M. Artetxe, M. Amutio, J. Bilbao, M. Olazar, Thermochemical routes for the valorization of waste polyolefinic plastics to produce fuels and chemicals. A review, Renewable and Sustainable Energy Reviews, 73 (2017) 346-368.

[15] M. Arabiourrutia, G. Lopez, M. Artetxe, J. Alvarez, J. Bilbao, M. Olazar, Waste tyre valorization by catalytic pyrolysis – A review, Renewable and Sustainable Energy Reviews, 129 (2020) 109932.

[16] F. Wang, N. Gao, C. Quan, G. López, Investigation of hot char catalytic role in the pyrolysis of waste tires in a two-step process, Journal of Analytical and Applied Pyrolysis, 146 (2020) 104770.

[17] M. Al-asadi, N. Miskolczi, Pyrolysis of polyethylene terephthalate containing real waste plastics using Ni loaded zeolite catalysts, IOP Conference Series: Earth and Environmental Science, 154 (2018) 012021.

[18] P. Das, P. Tiwari, Thermal degradation study of waste polyethylene terephthalate (PET) under inert and oxidative environments, Thermochimica Acta, 679 (2019) 178340.

[19] F. Awaja, D. Pavel, Recycling of PET, European Polymer Journal, 41 (2005) 1453-1477.

[20] A. Dhahak, C. Grimmer, A. Neumann, C. Rüger, M. Sklorz, T. Streibel, R. Zimmermann, G. Mauviel, V. Burkle-Vitzthum, Real time monitoring of slow pyrolysis of polyethylene terephthalate (PET) by different mass spectrometric techniques, Waste Management, 106 (2020) 226-239.

[21] D. Kawecki, P.R.W. Scheeder, B. Nowack, Probabilistic Material Flow Analysis of Seven Commodity Plastics in Europe, Environmental Science & Technology, 52 (2018) 9874-9888.

[22] J. Lee, T. Lee, Y.F. Tsang, J.-I. Oh, E.E. Kwon, Enhanced energy recovery from polyethylene terephthalate via pyrolysis in CO2 atmosphere while suppressing acidic chemical species, Energy Conversion and Management, 148 (2017) 456-460.

[23] A.M. Al-Sabagh, F.Z. Yehia, D.R.K. Harding, G. Eshaq, A.E. ElMetwally, Fe3O4-boosted MWCNT as an efficient sustainable catalyst for PET glycolysis, Green Chemistry, 18 (2016) 3997-4003.

[24] S.-Y. Oh, T.-C. Seo, Upgrading biochar via co-pyrolyzation of agricultural biomass and polyethylene terephthalate wastes, RSC Advances, 9 (2019) 28284-28290.

[25] D. Oh, H.W. Lee, Y.-M. Kim, Y.-K. Park, Catalytic pyrolysis of polystyrene and polyethylene terephthalate over Al-MSU-F, Energy Procedia, 144 (2018) 111-117.

[26] S.O. Ayodeji, T.O. Oni, Thermal pyrolysis production of liquid fuel from a mixture of polyethylene terephthalate and polystyrene, Heat Transfer-Asian Research, 48 (2019) 1648-1662.

[27] A. Brems, J. Baeyens, C. Vandecasteele, R. Dewil, Polymeric Cracking of Waste Polyethylene Terephthalate to Chemicals and Energy, Journal of the Air & Waste Management Association, 61 (2011) 721-731.

[28] G. Ganeshan, K.P. Shadangi, K. Mohanty, Degradation kinetic study of pyrolysis and co-pyrolysis of biomass with polyethylene terephthalate (PET) using Coats–Redfern method, Journal of Thermal Analysis and Calorimetry, 131 (2018) 1803-1816.

[29] R.K. Mishra, A. Sahoo, K. Mohanty, Pyrolysis kinetics and synergistic effect in co-pyrolysis of Samanea saman seeds and polyethylene terephthalate using thermogravimetric analyser, Bioresource Technology, 289 (2019) 121608.

[30] https://www.akts.com/akts-thermokinetics-tga-dsc-dta-tma-ftir-ms/akts-thermokinetics-discontinuous-help-e-learning.html, accessed 10-05-2020 at 11 am.

[31] S. Vyazovkin, K. Chrissafis, M.L. Di Lorenzo, N. Koga, M. Pijolat, B. Roduit, N. Sbirrazzuoli, J.J. Suñol, ICTAC Kinetics Committee recommendations for collecting experimental thermal analysis data for kinetic computations, Thermochimica Acta, 590 (2014) 1-23.

[32] A.I. Osman, A. Abdelkader, C.R. Johnston, K. Morgan, D.W. Rooney, Thermal Investigation and Kinetic Modeling of Lignocellulosic Biomass Combustion for Energy Production and Other Applications, Industrial & Engineering Chemistry Research, 56 (2017) 12119-12130.

[33] A. Dhahak, G. Hild, M. Rouaud, G. Mauviel, V. Burkle-Vitzthum, Slow pyrolysis of polyethylene terephthalate: Online monitoring of gas production and quantitative analysis of waxy products, Journal of Analytical and Applied Pyrolysis, 142 (2019) 104664.

[34] Y.-K. Park, J. Jung, S. Ryu, H.W. Lee, M.Z. Siddiqui, J. Jae, A. Watanabe, Y.-M. Kim, Catalytic co-pyrolysis of yellow poplar wood and polyethylene terephthalate over two stage calcium oxide-ZSM-5, Applied Energy, 250 (2019) 1706-1718.

[35] B. Saha, A.K. Ghoshal, Model-Fitting Methods for Evaluation of the Kinetics Triplet during Thermal Decomposition of Poly(ethylene terephthalate) (PET) Soft Drink Bottles, Industrial & Engineering Chemistry Research, 45 (2006) 7752-7759.

[36] Z. Yao, S. Yu, W. Su, W. Wu, J. Tang, W. Qi, Kinetic studies on the pyrolysis of plastic waste using a combination of model-fitting and model-free methods, Waste Management & Research, 38 (2020) 77-85.

[37] S.A. Jenekhe, J.W. Lin, B. Sun, Kinetics of the thermal degradation of polyethylene terephthalate, Thermochimica Acta, 61 (1983) 287-299.

[38] J.D. Cooney, M. Day, D.M. Wiles, Thermal degradation of poly(ethylene terephthalate): A kinetic analysis of thermogravimetric data, Journal of Applied Polymer Science, 28 (1983) 2887-2902.

[39] S.R. Horton, J. Woeckener, R. Mohr, Y. Zhang, F. Petrocelli, M.T. Klein, Molecular-Level Kinetic Modeling of the Gasification of Common Plastics, Energy & Fuels, 30 (2016) 1662-1674.

[40] H. Li, Y. Tan, M. Ditaranto, J. Yan, Z. Yu, Capturing CO_2 from Biogas Plants, Energy Procedia, 114 (2017) 6030-6035.

[41] I. Martín-Gullón, M. Esperanza, R. Font, Kinetic model for the pyrolysis and combustion of poly-(ethylene terephthalate) (PET), Journal of Analytical and Applied Pyrolysis, 58-59 (2001) 635-650.

[42] S. Kumagai, R. Yamasaki, T. Kameda, Y. Saito, A. Watanabe, C. Watanabe, N. Teramae, T. Yoshioka, Tandem μ-reactor-GC/MS for online monitoring of aromatic hydrocarbon production via CaO-catalysed PET pyrolysis, Reaction Chemistry & Engineering, 2 (2017) 776-784.

[43] N. Sophonrat, L. Sandström, A.-C. Johansson, W. Yang, Co-pyrolysis of Mixed Plastics and Cellulose: An Interaction Study by Py-GC×GC/MS, Energy & Fuels, 31 (2017) 11078-11090.

[44] A.I. Osman, Mass spectrometry study of lignocellulosic biomass combustion and pyrolysis with NOx removal, Renewable Energy, 146 (2020) 484-496.

[45] M. Artetxe, G. Lopez, M. Amutio, G. Elordi, M. Olazar, J. Bilbao, Operating Conditions for the Pyrolysis of Poly-(ethylene terephthalate) in a Conical Spouted-Bed Reactor, Industrial & Engineering Chemistry Research, 49 (2010) 2064-2069.

[46] M. Dzi□cioł, J. Trzeszczyński, Temperature and atmosphere influences on smoke composition during thermal degradation of poly(ethylene terephthalate), Journal of Applied Polymer Science, 81 (2001) 3064-3068.

[47] T. Yoshioka, G. Grause, C. Eger, W. Kaminsky, A. Okuwaki, Pyrolysis of poly(ethylene terephthalate) in a fluidised bed plant, Polymer Degradation and Stability, 86 (2004) 499-504.

[48] D. Garozzo, M. Giuffrida, G. Montaudo, R.W. Lenz, Mass spectrometric characterization of poly(ethylene terephthalate-co-p-oxybenzoate), Journal of Polymer Science Part A: Polymer Chemistry, 25 (1987) 271-284.

Figures

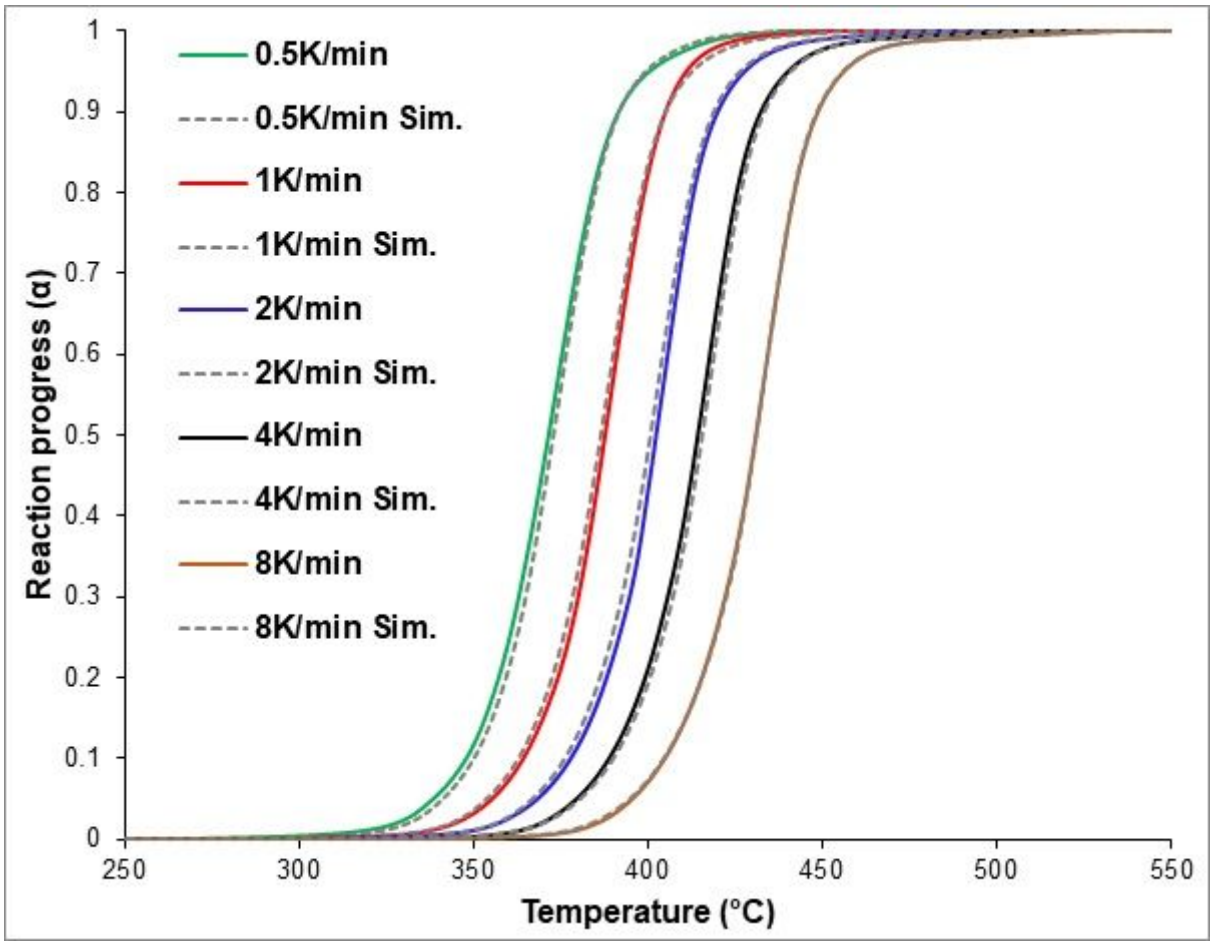

Figure 1

Reaction progress (α) versus the temperature for the PET pyrolysis where the coloured and dashed grey curves show the practical and theoretical calculations, respectively.

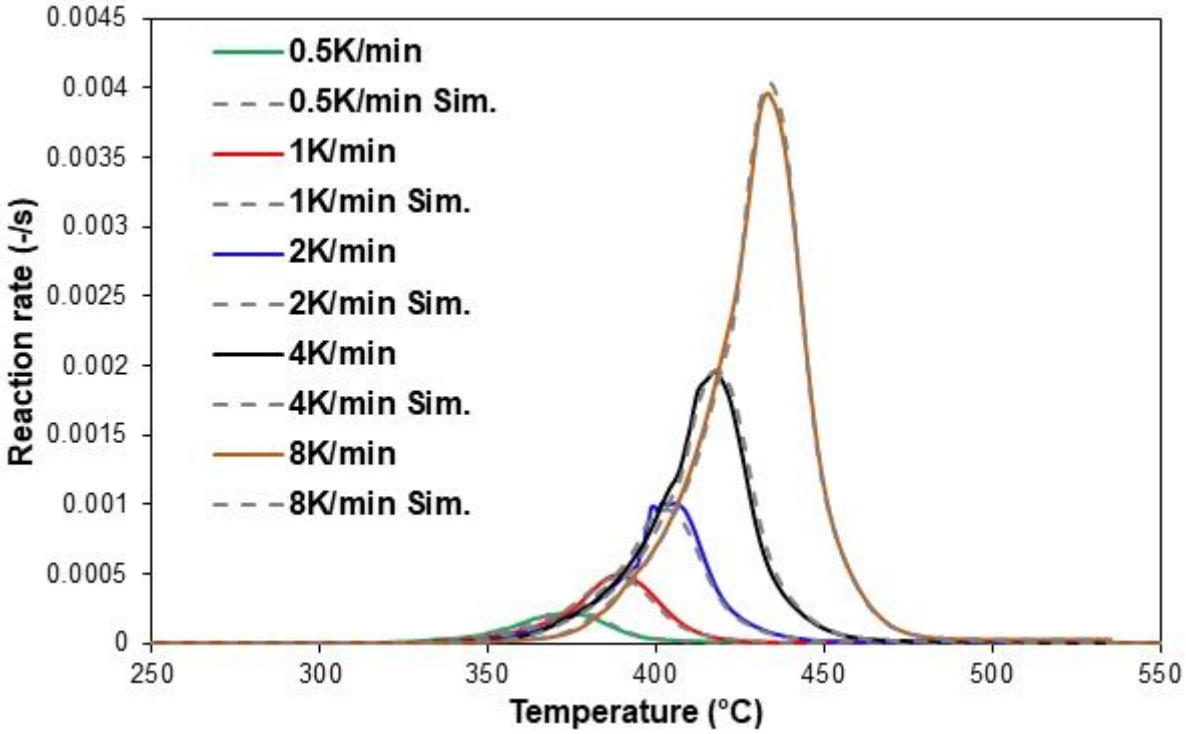

Figure 2

Reaction rate versus the temperature for the PET pyrolysis where the coloured and dashed grey curves show the practical and theoretical calculations, respectively.

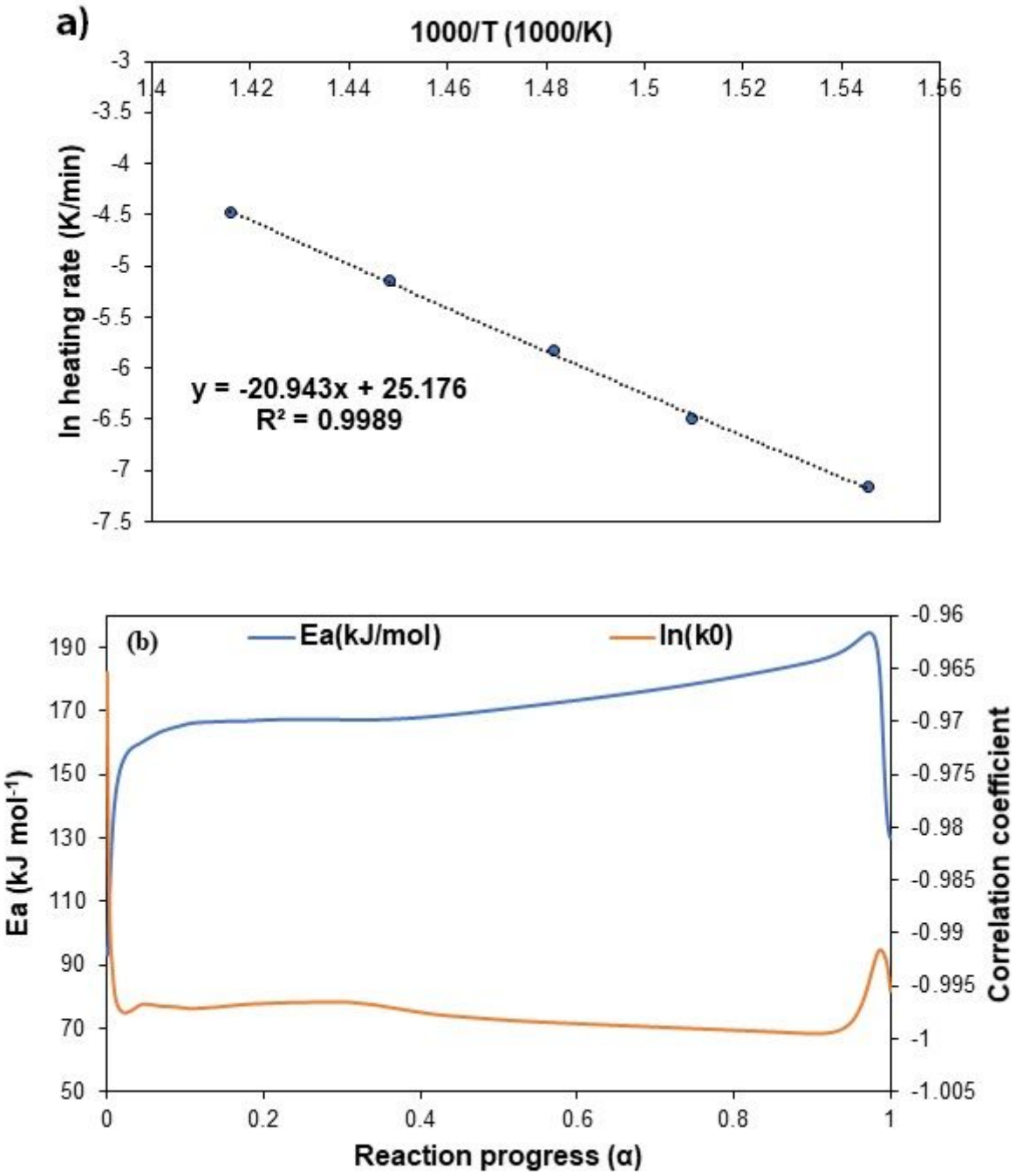

Figure 3

Kinetic parameters calculated by different methods (a) Ea using the ASTM-E698 method and (b) Ea using the Flynn-Wall and Ozawa (FWO) method for the PET pyrolysis.

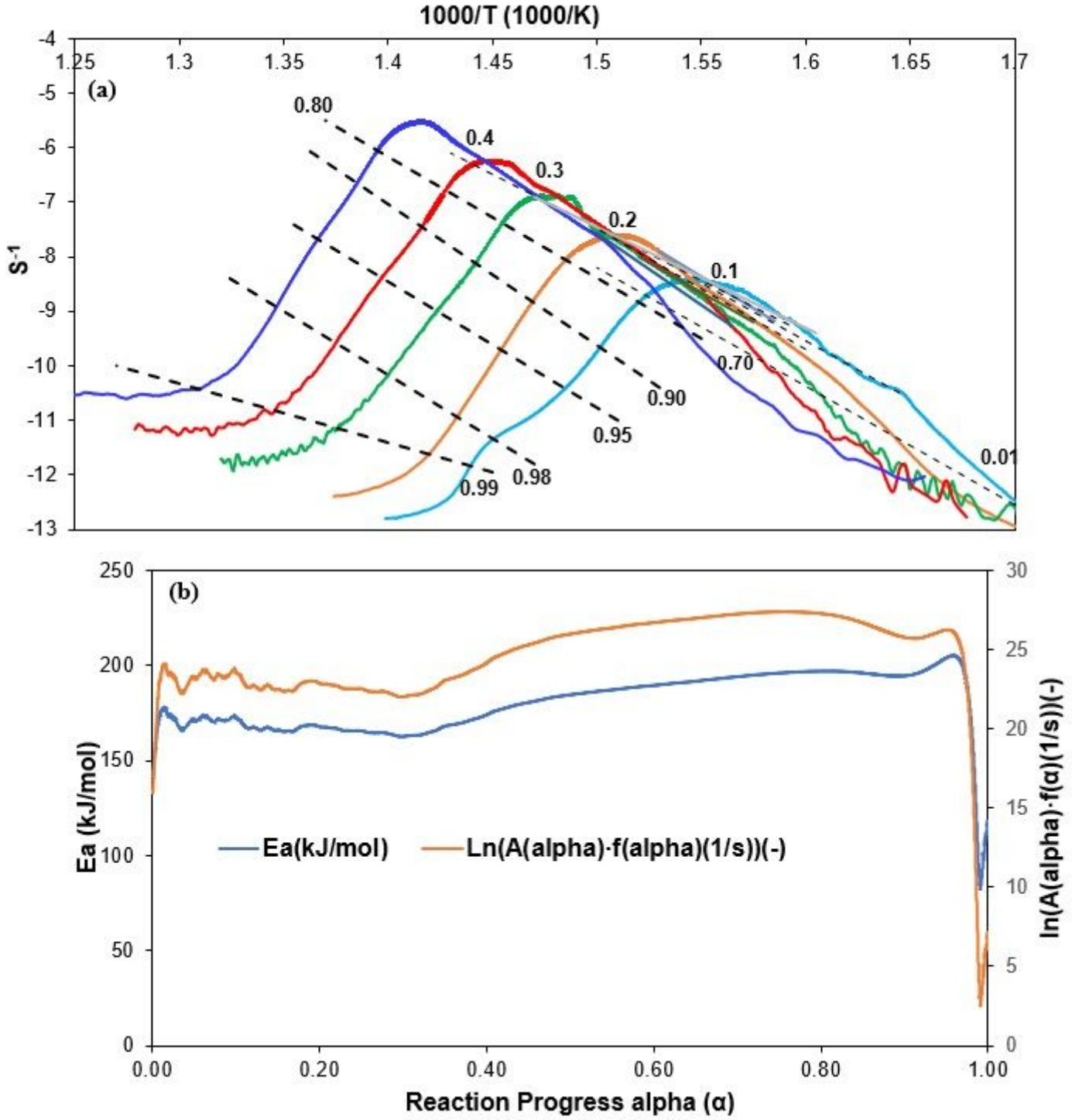

Figure 4

Kinetic parameters calculated with the differential iso-conversional, a) Natural logarithm of the reaction rate in (s-1) versus the inverse temperature, b) Ea and ln k0.

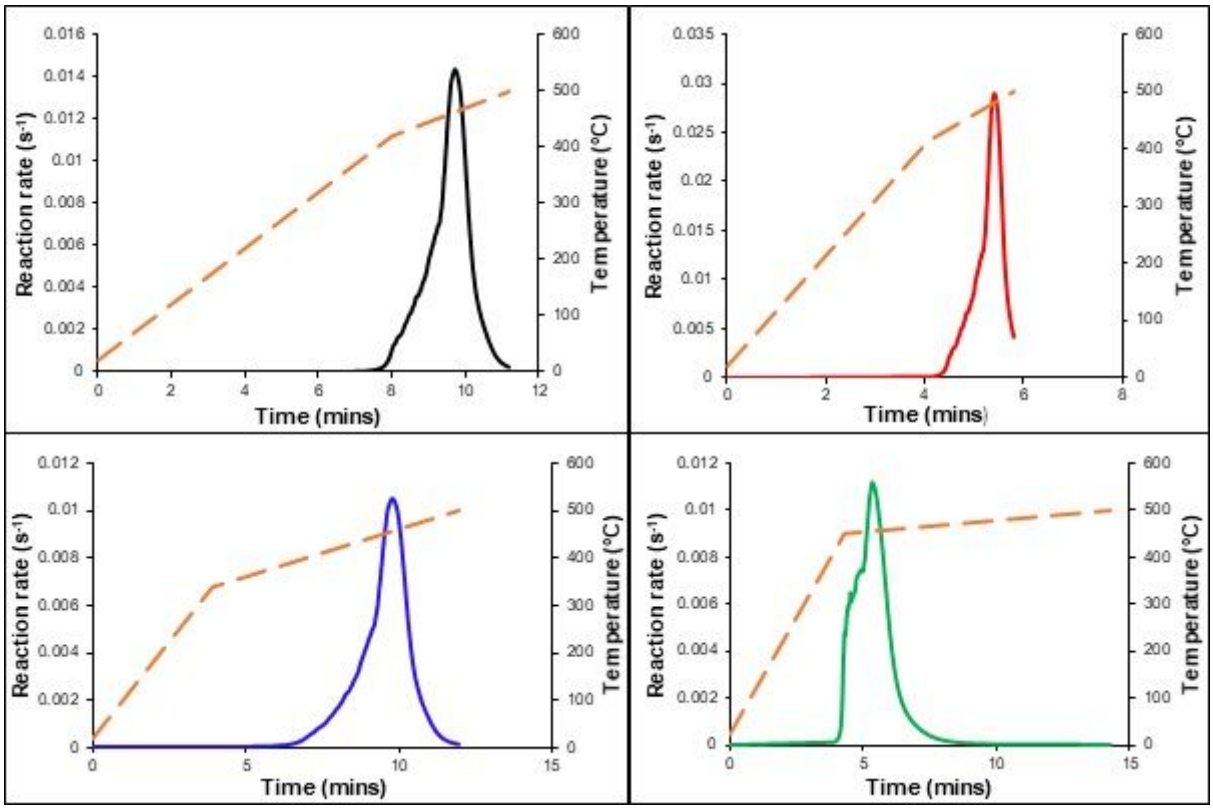

Figure 5

Prediction of PET pyrolysis at different temperature and heating rates (a-d) using a step-based heating regime.

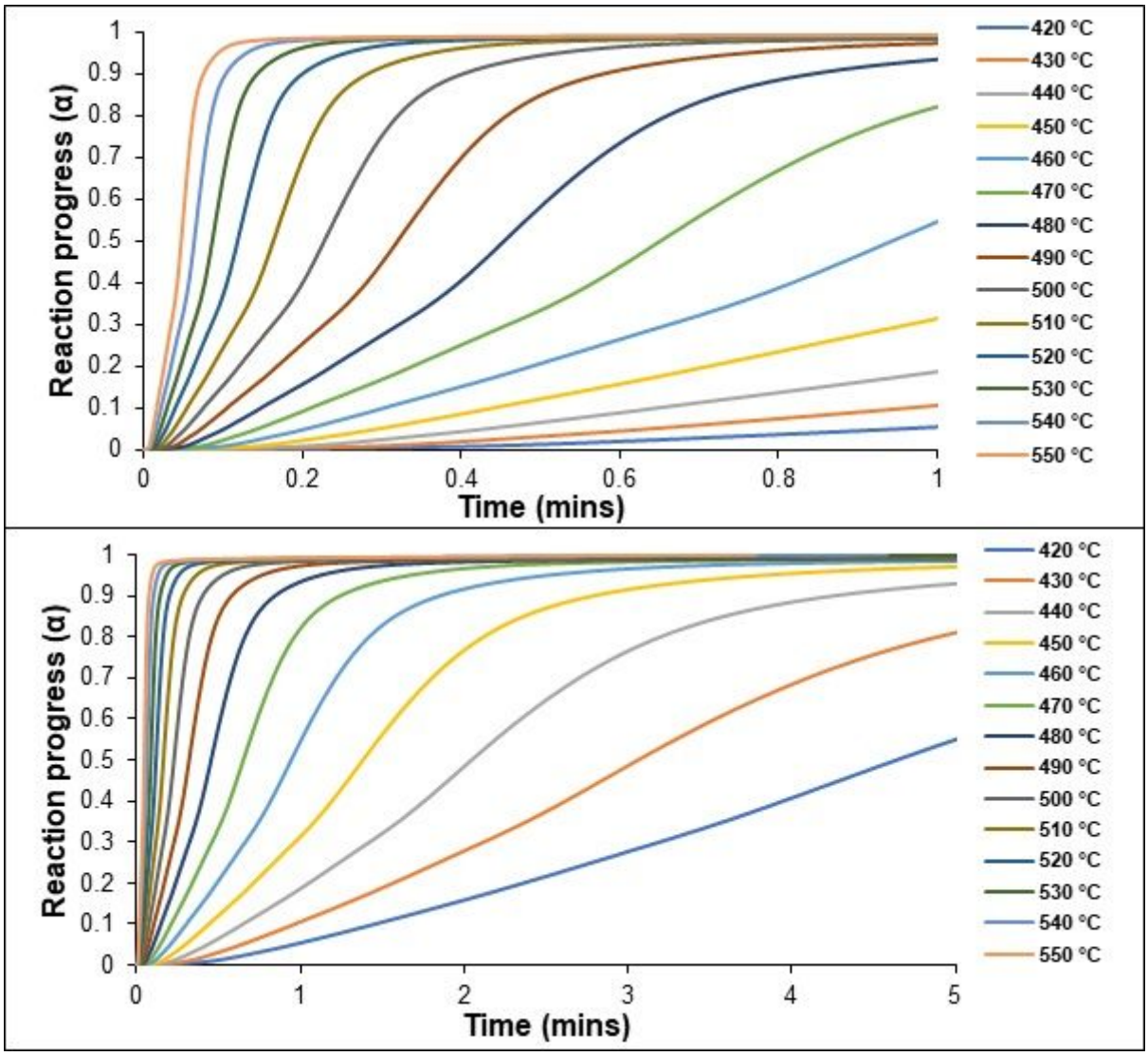

Figure 6

The isothermal prediction of PET pyrolysis showing 14 isotherms and the change in reaction progress against time in the temperature range of 420-550 °C and time range of 1 and 5 minutes, respectively.

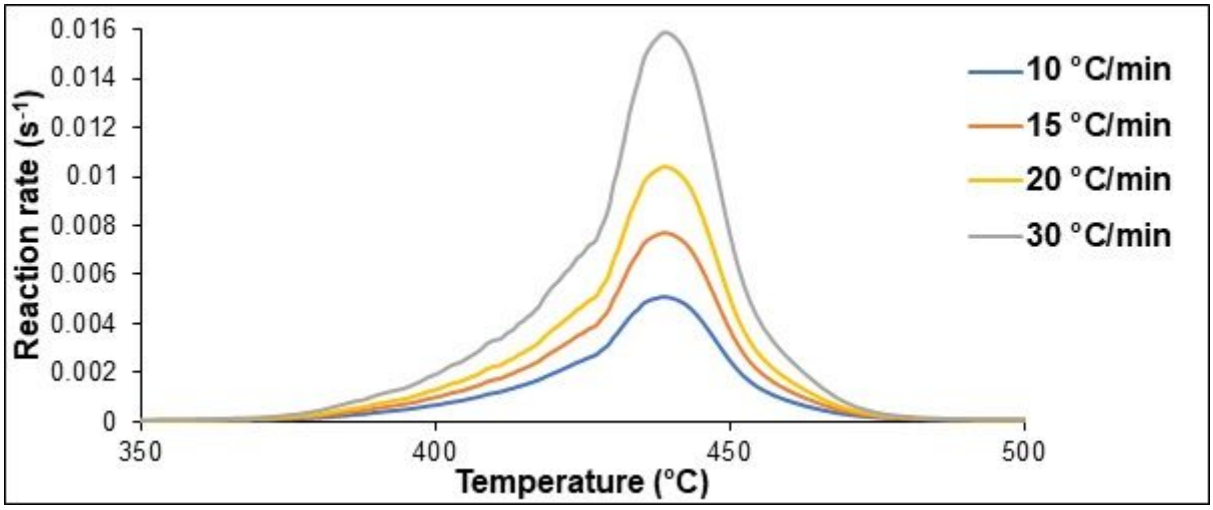

Figure 7

The non-isothermal prediction of PET pyrolysis under a non-isothermal heating regime at higher heating rates of 10, 15, 20 and 30 oC.min-1 using AKTS thermokinetics software.

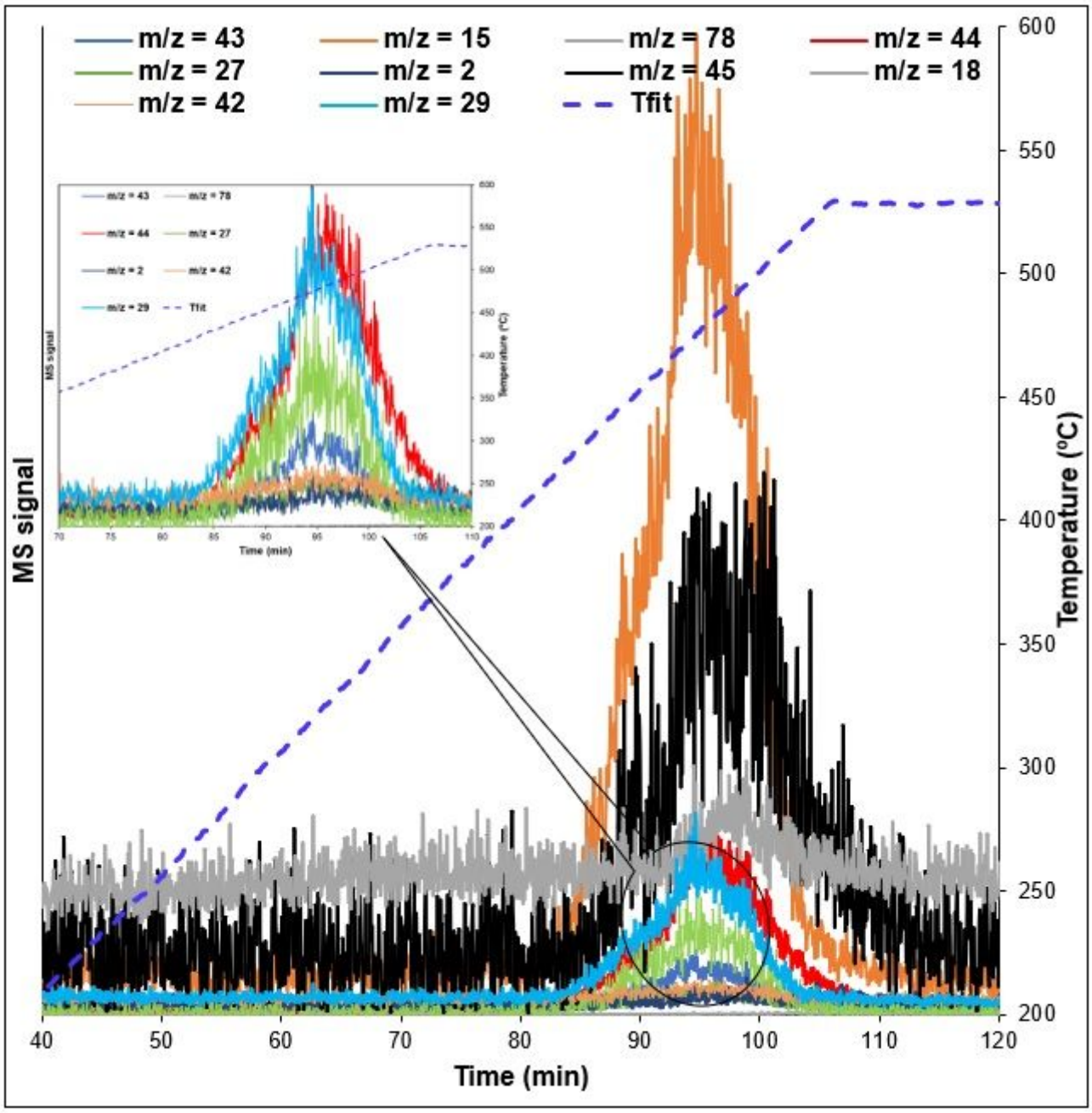

Figure 8

Mass spectrum profile of the evolved gaseous emissions during the PET pyrolysis under N2 atmosphere for temperature up to 530 °C with a heating rate of 5 °C.min-1. The blue-dashed line represents the temperature recorded via the thermocouple.

Supplementary Files

This is a list of supplementary files associated with this preprint. Click to download.

- GraphicalAbstract.jpg
- Equations.pdf
- ESIrevised.pdf
- ESEUD2000099.zip